The International Journal of Advanced Manufacturing Technology
https://doi.org/10.1007/s00170-023-10881-9

ORIGINAL ARTICLE

Mechanical characterization of high volume fraction Al7075-Al_2O_3 composite fabricated by semisolid powder processing

Saeed Aghajani[1] · Vahid Pouyafar[1] · Ramin Meshkabadi[2] · Alex A. Volinsky[3] · Amir Bolouri[4]

Received: 1 July 2022 / Accepted: 11 January 2023

Abstract

The mechanical properties and physical characteristics of aluminum alloy composites can be significantly improved by adding reinforcing phases. However, the high loading of the reinforcement phase in Al7075-Al_2O_3 composites has not been thoroughly studied. In this work, a combination of semisolid metal powder processing and powder metallurgy is used to process and manufacture Al7075-Al_2O_3 composites with a high reinforcement fraction of > 40 vol.%. The effects of processing parameters on the microstructures and mechanical properties of the composite material are discussed in detail. The loading limits of the high volume Al_2O_3 reinforcement in Al7075 composites are identified and linked to the processing parameters. A methodology is introduced to estimate the consolidation temperature of Al7075 alloy using compaction testing. Al_2O_3 particles (the average particle size of 120 μm) were mechanically milled with Al7075 powder (the average particle size of 20 μm) for 10 min and 5 h using a high-energy planetary ball mill. The mixture was then compacted in the semisolid state at 615 °C under the compaction pressures of 50 MPa and 100 MPa. By increasing the milling time from 10 min to 5 h, the deformation of aluminum powders and the fracture of Al_2O_3 reinforcement particles occur, restricting the loading limit of reinforcement. The milling time also shows a dominant effect on the powder morphology, microstructure, and mechanical properties of Al7075-Al_2O_3 composites. Increasing compaction pressure from 50 to 100 MPa significantly improved the compressive strength of the composite from 218 to 652 MPa. Al7075-Al_2O_3 composite with 40 vol.% of reinforcing phase exhibits the highest hardness of 198.2 HV and 96.9% relative density when it is milled for 5 h and compacted at 100 MPa. However, this composite shows the highest strength of 652 MPa when it is milled for 10 min. By increasing the reinforcing phase to 50 vol.% and 60 vol.%, the hardness, density, and compressive strength of composites decreased. The composites with 60 vol.% of reinforcing phase appeared overloaded. Results show that semisolid metal powder processing has huge potential for the fabrication of high loading Al_2O_3 in Al7075 matrix with near theoretical density.

Keywords Al7075/Al_2O_3 composite · Mechanical characterization · Semisolid powder processing · Powder metallurgy

✉ Amir Bolouri
Amir.Bolouri@UWE.AC.UK

Saeed Aghajani
s.aghajani94@ms.tabrizu.ac.ir

Vahid Pouyafar
pouyafar@tabrizu.ac.ir

Ramin Meshkabadi
r_meshkabadi@uma.ac.ir

Alex A. Volinsky
volinsky@eng.usf.edu

[1] Department of Manufacturing Engineering, University of Tabriz, Tabriz 51666-16471, Iran

[2] Department of Engineering Sciences, Faculty of Advanced Technologies, University of Mohaghegh Ardabili, Namin 56318-44133, Iran

[3] Department of Mechanical Engineering, University of South Florida, Tampa, FL 33620, USA

[4] School of Engineering, University of the West of England, Bristol, UK

Published online: 23 January 2023

1 Introduction

Aluminum alloys are popular lightweight alloys used in different applications due to their desirable properties. Among them, the 7000 Al series are more appealing because of the high fracture toughness and high resistance to stress corrosion cracking [1]. Good performance justifies the high cost of this alloy compared to others. Despite many standard applications, conventional materials do not satisfy the wide range of expectations. Consequently, aluminum-based metal composites reinforced with hard ceramic materials are fabricated for catering the demands of automotive, aerospace, and military industries [2, 3].

High strength with low mass are needed for structural materials applications. Adding a high volume fraction of particles can double the elastic modulus and strength of the matrix alloy [4]. Low coefficient of thermal expansion and improved thermal conductivity are some advanced characteristics of highly loaded ceramics [4]. The composites of aluminum alloys with a high volume of reinforcement (> 40vol%) have widespread applications in sporting goods, automotive engineering, aerospace industry, and defense technology [5, 6]. Aluminum matrix composites containing high volume fraction ceramic particles are also being used as microprocessor lids and integrated heat sinks in electronic packaging. They are also used as carrier plates and microwave housing [7]. Although the addition of more than 30% by volume of ceramic reinforcing particles is not recommended for structural applications due to reduced material ductility, it has been shown that aluminum matrix composites containing more than 50% by volume of reinforcing particles can be strong and relatively ductile which justifies their use [4, 8, 9].

There has been research conducted on the manufacturing methods of high volume fraction composites through casting [7, 10], powder metallurgy [11], and infiltration [12]. Despite improved properties of this kind of composites, there are limitations such as compositional control in casting and sintering balance [13], ceramic powder percolation in powder metallurgy [14], and closed and half closed pore problems in infiltration casting [15]. However, the major concern shared by all methods is wettability and uniform dispersion of ceramic particles [16, 17]. Recently, Jiang e al. [18] and Zhu et al. [19] prepared SiC/Al6082 aluminum matrix composites by squeeze casting and squeeze casting combined with stir casting, respectively. It was shown that SiC content and squeeze casting parameters had significant impacts on the microstructure and mechanical properties of the 6082 aluminum alloy.

To achieve a uniform distribution of the reinforcement phase and the possibility of producing complex-shaped components with large dimensions, the combined process of powder metallurgy and semisolid forming can be used. Powder metallurgy is one the manufacturing methods of metal matrix composites in a solid state, which causes the uniform distribution of particles within the matrix [20]. It is less likely to form intermetallic phases in powder metallurgy [21]. Semisolid powder processing (SPP) is a novel technology that combines powder metallurgy and semisolid metal forming [22]. The ability of SPP in terms of uniform distribution of reinforcement by mechanical milling has been demonstrated [23]. A method that has the advantages of powder metallurgy and semisolid forming methods is very important for the industrial production. For example, Javdani et al. [24] used blended powder semisolid forming to fabricate Al7075/Al_2O_3 composites and eliminate the drawbacks of conventional semisolid powder metallurgy. They fabricated the Al7075/Al_2O_3 metal matrix composites for the first time using this method.

The SPP has been successfully applied in the processing of composite materials such as Al-Cu reinforced with h-BN [25], Al6061 with SiC [26] and Al7075 with 5, 10, and 20 wt.% of Al_2O_3 [24]. However, to the best of our knowledge, the SPP of Al 7075/Al_2O_3 for high loading reinforcement of > 40 vol.% has not been reported yet. Al_2O_3 is one of the common ceramics used as a reinforcing phase in metal matrix composites. Due to the working temperature in the SPP method and the high thermal stability of this phase [27], it was used as a reinforcement in this research.

It has been widely proven that the matrix microstructure and its consequent mechanical properties have a considerable influence on the overall performance of the composites [28, 29]. The matrix structure strongly depends on the semisolid forming temperature. Although it has been more than 30 years since the introduction of SPP, no in-depth research has been conducted concerning the optimal semisolid forming temperature and high reinforcement loading limit of Al_2O_3 in Al7075. Understanding the role of various materials and process parameters on the properties of the final product is the essential step in the evaluation of the suitability of such composites for industrial applications. To the best of our knowledge, few studies have been conducted to fabricate the high-loading Al_2O_3-Al7075 composites. The objective of the present study is to determine the optimal SPP temperature for Al7075 matrix composites and prepare composite powder with uniform dispersion of high-volume fraction reinforcing phase. Then, a sample is manufactured using SPP to demonstrate the effectiveness of the method to achieve the desired mechanical properties.

In this study, Al7075/Al_2O_3 composites with reinforcement loadings of > 40 vol.% were manufactured by a combination of semisolid processing and powder metallurgy. Since the mechanical properties of metal matrix composites are a function of the production parameters [30], the effects of reinforcement volume fraction, milling time, and compaction pressure on the microstructure, mechanical properties, microhardness, and density were investigated.

2 Materials and methods

2.1 Preparation of Al7075 powder

Al7075 elemental powder alloy was used as the base material. High purity (99.96%) gas atomized aluminum powder (Khorasan Powder Metallurgy Company, Iran) with an average size of 20 μm was used as the starting material. The constituents and characteristics of the Al7075 powder are presented in Table 1. Elements of the Al7075 alloy were sufficiently supplied to the ethanol shower and became ultrasonic at 25 kHz frequency and 23 °C. After half an hour of homogenizing, the mixture was placed into a resistance oven to vaporize the solution. Then, dried powders were mechanically alloyed in a mechanical ball mill machine for 5 h, leading to a homogeneous alloy.

2.2 Preparation of Al7075/Al_2O_3 powder composite

Semispherical Al_2O_3 powders (Iran Alumina Company, Iran) with an average size of 120 μm were used as the reinforcement. The blending process of the Al7075 with different amounts of Al_2O_3 (40, 50, and 60 vol.%) was executed with a high energy planetary ball mill. The stainless steel balls used had 10 mm and 15 mm diameters. The ball-to-powder weight ratio was approximately 5:1 and the mill rotated at 250 rpm. Composite powders were divided into two parts, one milled for 10 min and the other for 5 h. To avoid any unjustified cold welding and clustering of milled particles, stearic acid, as a process control agent, was added at 2.5 wt.% of the total powder charge. The powder composite samples were dried in the air after mixing.

2.3 Determining the appropriate semisolid temperature

MoS_2 was sprayed on the die wall and the punch for lubrication in order to reduce die wall friction effects. Al7075 powder samples were weighed and poured into the die cavity to be compacted at different temperatures (575, 585, 595, 605, 615, and 625 °C). For each specimen, 12 g powder was used to fill the die cavity. The prepared powders were fed into the die and placed inside the PID controlled furnace. The temperature control was within ± 2 °C. The samples were cold compacted under 10 MPa to produce a weakly bound substance.

Then, the set was fixed inside a screw-driven universal testing machine. The die and powders were heated in the furnace, while the load and displacement of upper ram were controlled and measured by the testing system. Once the material was heated to the desired semisolid temperature, the upper ram moved down at a velocity of 0.07 mm/s and compressed the semisolid powder. To accurately measure the furnace and powder temperatures, two K-type thermocouples were embedded inside the furnace and die set hole. A uniaxial constant compressive pressure of 50 MPa was applied at indicated semisolid temperature. The applied pressure was held for 45 min to equalize the temperature and the pressure. Fabricating parameters including compaction pressure, holding time, and punch velocity were selected in accordance with the previous experimental studies [23, 24].

The machine was equipped with a closed-loop control system to stabilize the pressure within the experiment period. All samples were cooled inside the furnace after removing the pressure. The experimental layout is shown in Fig. 1. The unit consists of an electrical furnace, a temperature control unit, and a load cell. Table 2 lists fabricated Al7075/Al_2O_3 composite samples with the process parameters.

The effects of semisolid temperature, density and compressive strength of the fabricated samples were evaluated, and finally, the appropriate semisolid temperature was determined.

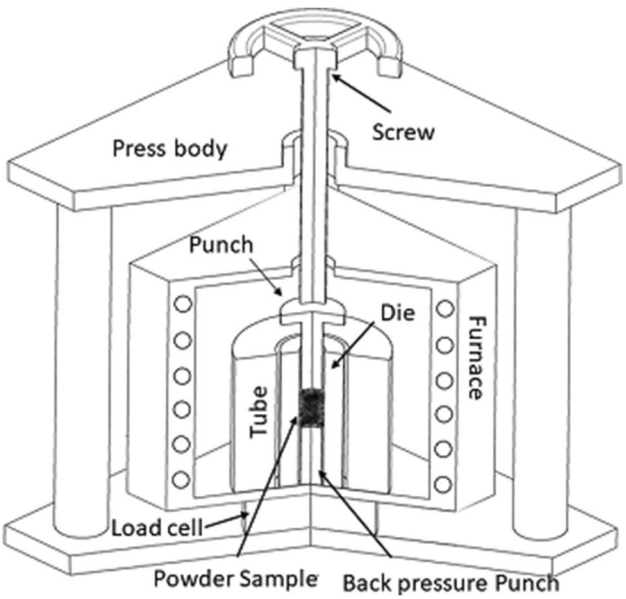

Fig. 1 Experimental layout of the semisolid compaction process

Table 1 Elemental 7075 powder constituents and particle size

Element	Al	Zn	Mg	Cu	Cr	Fe	Si	Mn
Content (%)	Balance	5.6	2.5	1.5	0.23	0.2	0.1	0.1
Particle size (μm)	20	20	63	45	63	45	5	63

2.4 Fabrication of Al7075/Al_2O_3 composite by SPP

The milled Al7075/Al_2O_3 powders were weighed and poured into the forging die and placed inside the furnace. The same procedure used in Section 2.3 was carried out for the composite samples. This time, all the experiments were carried out at the appropriate temperature specified in the previous section. The pressure (50 MPa or 100 MPa) was then slowly applied and kept for 45 min. The cooling and pressure removal processes were exactly like the former experiments.

3 Results and discussion

3.1 Semisolid temperature characteristics

The microstructure evolution of aluminum powder in the semisolid region can be divided into three stages: the initial coarsening of the grains within powders, the formation of the continuous liquid layer on the particle surface, and the final slight coarsening [31]. At semisolid temperature intervals, alloying elements are concentrated in the liquid phase. By varying the semisolid process temperature, not only the liquid fraction, but also the composition of the liquid phase can be controlled. In other words, the enrichment of alloying elements, which influences the mechanical properties of the alloy, differs in the liquid phase [32]. In addition, a dense matrix with high strength could improve composite properties. The optimized semisolid temperature with an efficient liquid fraction was investigated for the elemental Al7075 alloy at different remelting temperatures of 575, 585, 595, 605, 615, and 625 °C. The proportional liquid fraction from Differential Scanning Calorimetry (DSC) analysis equals to 8, 14, 20, 31, 42, and 60%, respectively. The solidus and liquidus temperatures are 540 °C and 650 °C, accordingly.

The density of compacted samples was measured by using the Archimedes principle. Figure 2 shows the relative density of forged Al7075 elemental powder at different temperatures. The relative density was increased by increasing the temperature up to 615 °C. This is because the liquid phase flows and fills the pores and voids between the particles [23]. Therefore, the addition of liquid significantly assisted the densification of the powder mixture, and near full density was obtained. Although the sample's relative density in the semisolid region increased up to 615 °C (40% liquid fraction), but it decreased in the sample produced at 625 °C (60% liquid fraction). The liquid phase was squeezed out, which left solid particles to cluster over each other and decreased the density. Due to many solid particles, this phenomenon was more notable in high reinforcement loading composites [23].

Table 2 Variable experimental parameters used for the fabrication of Al7075/Al_2O_3 composites

Variable	Value
Al_2O_3 volume percentage	40%, 50%, and 60%
Milling time	10 min and 5 h
Semisolid compaction pressure	50 and 100 MPa

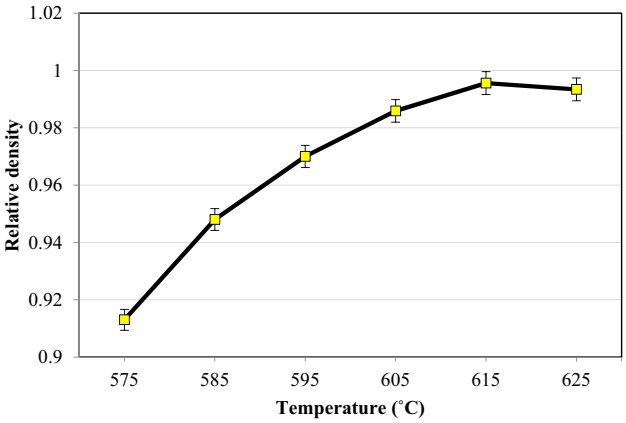

Fig. 2 Relative density vs. temperature diagram of forged Al7075 elemental powder under 50 MPa

The true compaction curves for the elemental 7075 Al alloys compacted at different semisolid temperatures are displayed in Fig. 3. The semisolid temperature had an impact on the mechanical behavior of the alloy. The compressive strength increased with temperature. As the liquid fraction increased, the compressive strength increased, as well. This is due to the increased amount of liquid phase, which provides better adhesion between grains at elevated temperatures. At temperatures higher than 605 °C, and the liquid fraction over 20%, the density and compressive strength were the highest. This is because of the increased amount of melting at the surface

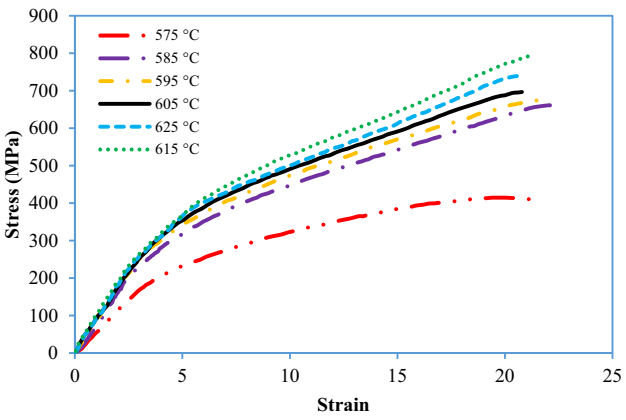

Fig. 3 True compression curves of Al7075 alloys compacted under 50 MPa at different temperatures

of Al particles rather than inside them [26]. This helps the liquid phase to flow better and fill any unwanted porosity generated in powder compaction. The ultimate compressive strength became almost steady at a liquid fraction of more than 40%. Similar compaction behavior is the possible reason for this phenomenon. By increasing the temperature to 625 °C, the strength slightly decreased because of the primary particles' growth. Also, due to the lack of liquid phase at low temperature, the primary particles were attached to each other and formed larger particles under the applied pressure. These results are in agreement with the previous works by Chen et al. [33, 34].

Despite higher relative density with increasing semisolid temperature, the distribution of liquid and solid phases became heterogeneous at more than 50% of the liquid phase [35]. In this case, segregation of liquid and solid phases caused agglomeration of solid particles. In composites, this situation results in clustering of reinforcement at the bottom of the die. For this reason, the proper temperature for manufacturing Al7075 base composites is 615 °C with a corresponding liquid fraction of 40%.

Figure 4 shows the scanning electron microscopy (SEM) of the Al7075 powder compacted at the optimal semisolid temperature of 615 °C and 50 MPa pressure. It is comprised of fine globular grains (bright phase) surrounded by a continuous liquid film (dark phase). These results suggest that the optimal temperature for semisolid compaction of Al7075 elemental powder can be 615 °C with a corresponding increase in density and compressive strength.

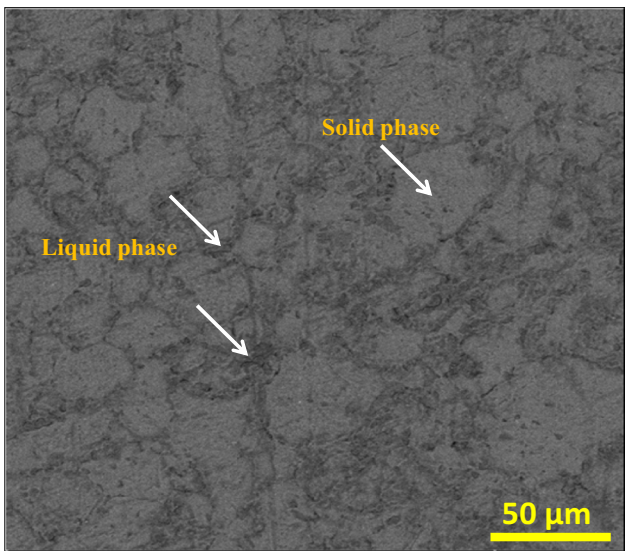

Fig. 4 The semisolid microstructure of Al7075 compacted at 615 °C and 50 MPa

3.2 Morphological changes and microstructure

It is evident that milling time has a significant influence on the powder morphology, which itself significantly affects the microstructure and mechanical properties of the manufactured composites. Figure 5 shows the powder morphology before and after the milling. Figure 5a, b show 20 µm Al7075 and 120 µm Al_2O_3 particles before milling. The major challenge related to metal matrix composites is the homogenous distribution of reinforcements within the matrix to achieve the defect-free microstructure [25]. It is due to the fact that a uniform distribution of reinforcements will result in composites with improved mechanical properties. However, a clustering of the reinforcement particles will be a major constraint which requires a careful synthesis method. The uniform distribution of alumina particles in Fig. 5c, achieved by planetary ball milling, eliminates this shortcoming. As seen in Fig. 5c, e, the milling duration had an enormous effect on the morphology of composite powder at high reinforcement loadings. To ensure that the homogenizing and alloying of 7075 aluminum alloy were successfully accomplished, energy dispersive spectroscopy (EDS) analysis was conducted. Figure 5g shows the dispersion of alloying elements in the microstructure of Al7075 alloy.

The powder particle size changes with the milling time. This is due to two opposing factors of cold welding and the fracture of powder particles. While the cold welding increases the particle size, the fracture reduces the size. In the early stages of milling, the powder particles are still soft and the cold welding predominates. Milling the powders for a short time does not make any noticeable changes in the morphology of the matrix and reinforcement particles (Fig. 5c). Thus, it could be claimed that no intensive alloying has happened and only the reinforcement particles were homogeneously dispersed between the matrix phase particles. Mixing with the ceramic particles also could increase the brittleness of Al7075 particles, and consequently, it increases the rate of fracture. Hence, with the continued milling, the particles get work hardened and become more brittle and their fracture leads to a reduction in the particle size. Thus, the rate of fracture tends to increase with increasing the milling time [36]. Large Al_2O_3 particles in 10 min milled composites are distributed between 20 µm aluminum particles. By increasing the milling time, the large and brittle alumina particles are simultaneously fractured with plastic deformation of soft Al particles (Fig. 5e). The observed microcracks in Fig. 5d are considered the nucleation sites for crack propagation. As a result, 120 µm Al_2O_3 particles decreased to an average size of 1 µm after 5 h of high energy planetary ball milling (Fig. 6). The difference in the size of ceramic particles after ball milling causes different changes in the morphology of composite powders [37]. It has been reported that the particle size is stabilized and does

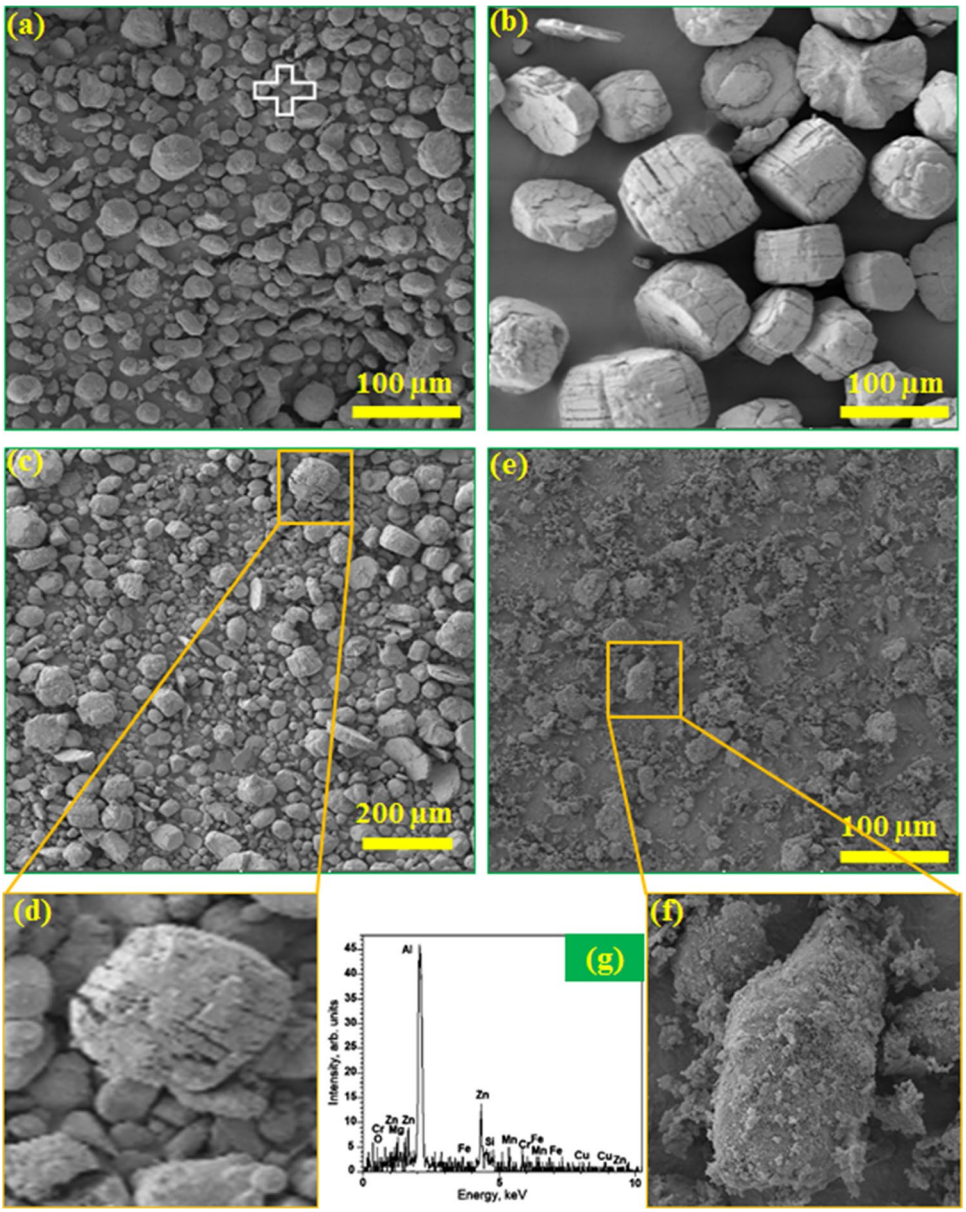

Fig. 5 SEM micrographs of powder morphology: **a** 7075 elemental alloy; **b** 120 µm Al_2O_3 particles; **c** 10 min milled composite powder; **d** alumina particle after milling; **e** 5 h milled composite powder; **f** magnified particle, **g** EDS analysis of the 7075 alloy in the marked region of **(a)**

not change with further milling [36]. Also, by comparing the morphology of aluminum particles before and after milling, these particles experienced plastic deformation and flattening. The reason is the acceleration of the milling process in the presence of alumina particles. Particle dispersion was successfully accomplished during 5 h milling, but the percentage of equiaxed grains was still less, and most of them were irregular. Despite the tendency of aluminum particles to plastic deformation and cold welding, the brittle alumina particles hindered their cohesion by fragmentation and adhesion to the surface of aluminum particles. Therefore, the distribution of Al_2O_3 particles was homogeneous in both cases. Once fracture occurred, fresh particle surfaces were produced, and due to the high reactivity of these surfaces, the cold welding again became predominant leading to an increased particle size, as depicted in Fig. 5(f) for a milling time of 5 h. Also, the agglomeration of fragmented particles on the aluminum particles is seen in some areas of Fig. 5f.

The microstructure along the forged direction in the cross-section of the Al7075-50 vol.% Al_2O_3 composite compacted under 100 MPa pressure at 615 °C is shown in Fig. 7. It contains uniformly distributed Al_2O_3 particles, which are attained from the morphology of powders after being milled. The microstructure of samples apart from the experimental situation is a function of the morphology of milled powders. As seen in Fig. 7a for 10 min milled samples, 120 µm Al_2O_3 particles remained almost intact and were homogeneously distributed in the matrix. The microstructure of composite samples with fragmented reinforcements reveals that their distribution is predominantly at grain boundaries and, to a

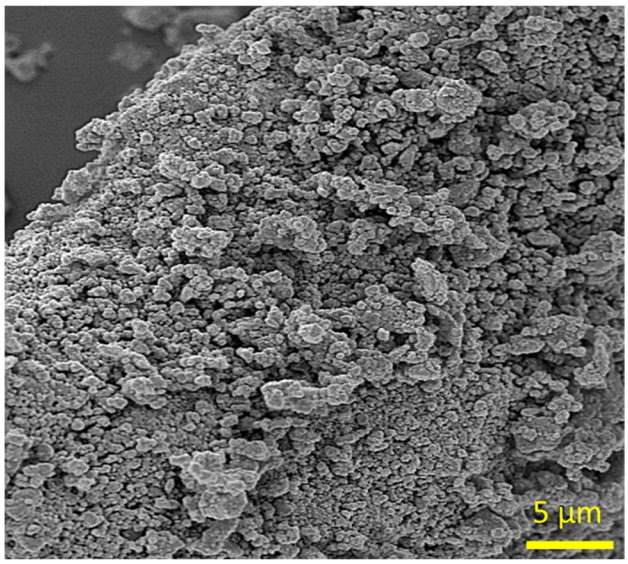

Fig. 6 Al_2O_3 particles after 5 h milling

less degree, at the matrix phase (Fig. 7b). This heterogeneous distribution is due to the adhesion of small broken particles to the surface of aluminum particles seen in Fig. 5e.

Figure 8 demonstrates the SEM micrographs of the samples compacted at 50 MPa and 100 MPa. Dark spots aligned with white arrows are pores between aluminum particles caused by less compression of spherical particles and solidification shrinkage. By comparing Fig. 8a, c, it is concluded that porosity is generated due to more solidification shrinkage in 10 min milled samples. Therefore, in high loading composites, small particles fill the matrix pores better. This conclusion is in agreement with Kang et al. studies [38]. Also, for both samples, the amount of porosity is decreased and more homogeneous distribution of the reinforcement is achieved by increasing the compaction pressure from 50 to 100 MPa (comparing Fig. 8a, c with Fig. 8b, d), which is due to the percolation of liquid phase between the attached alumina particles at high pressure. Additionally, the bond strength at the interface between the matrix and reinforcements can be improved. As shown in Fig. 8b for high loading composites, even at high pressure, the resistance of large particles against the flow of the liquid phase is more than that of the fragmented particles. As a result, the porosity of 10 min milled composites is higher than 5 h milled ones.

For analyzing the effect of high-volume fraction reinforcement on aluminum matrix composites, SEM micrographs of 60 vol.% Al_2O_3 are shown in Fig. 9. As seen in Fig. 9a, the surface of 5 h milled composites is full of black areas. These are empty spaces that belong to the reinforcement phase and are separated from the matrix in the surface preparation stage due to the weak bond strength. The solidification of primary aluminum dendrites causes the segregation of particles by the solid–liquid interface during consolidation process. This becomes more evident with the finer particles [27]. Thus, it can be concluded that the maximum reinforcement loading of these composites should be less than 60 vol.% and reach a maximum of 50 vol.%. In contrast, Fig. 9b relates to a 10 min milled composite with the same amount of reinforcement loading (60 vol.% fraction). Good distribution with proper consolidation is achieved for this composite. The main difference of this composite is the existence of microcracks on the reinforcement particles. The significant reason for cracking is the brittleness of alumina and low resistance to tension revealed in the solidification shrinkage. By increasing the volume of reinforcement, the pressure contribution of the soft matrix phase decreased. This situation when the matrix phase has

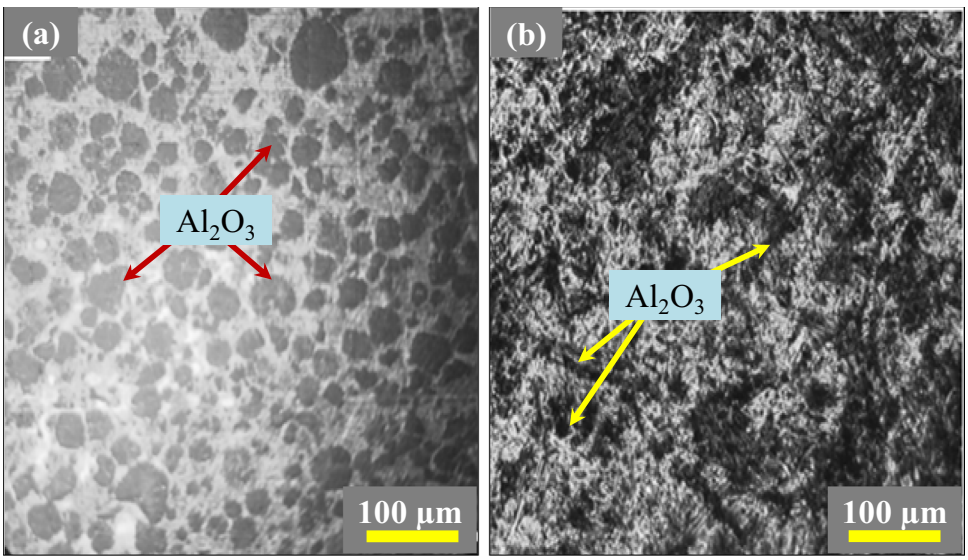

Fig. 7 Optical micrographs of forged samples with 50 vol.% Al_2O_3 milled for **a** 10 min and **b** 5 h and compacted under 100 MPa pressure at 615 °C

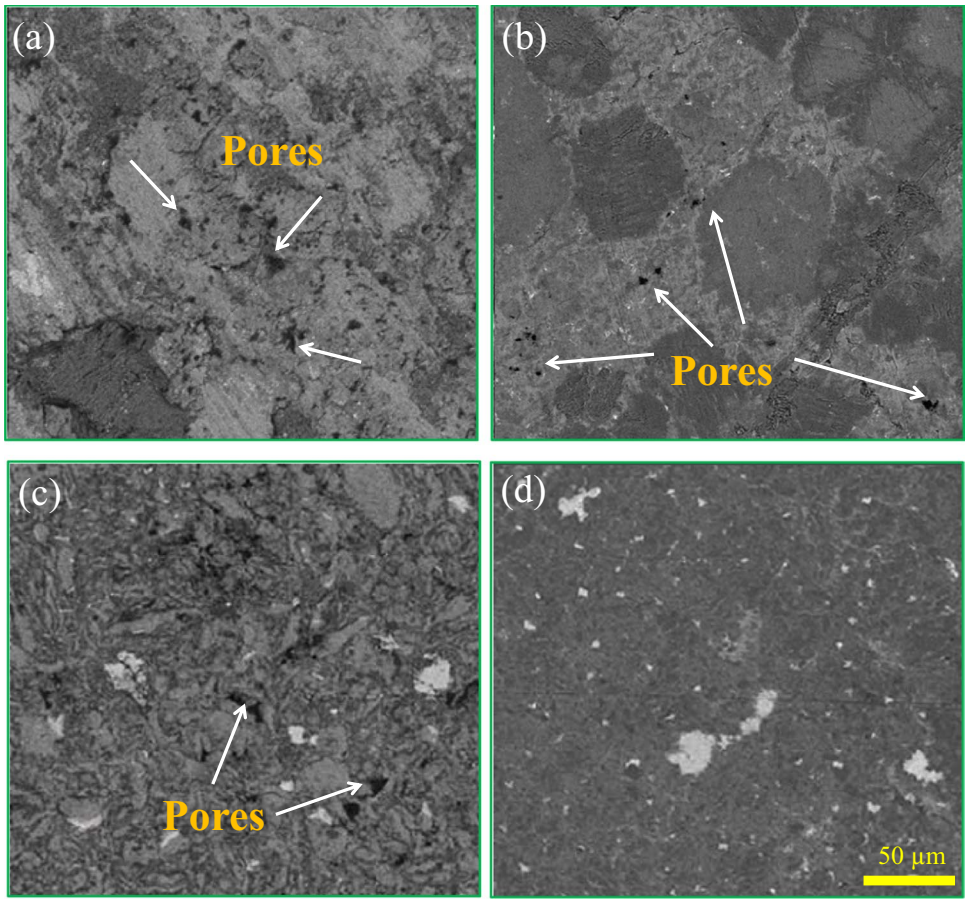

Fig. 8 SEM micrographs of Al7075/40 vol.% Al_2O_3 milled and compacted for **a** 10 min at 50 MPa, **b** 10 min at 100 MPa, **c** 5 h at 50 MPa, and **d** 5 h at 100 MPa

almost no contribution to the load-bearing capacity and just fills the cavities created by the alumina structure is called the loading limit [39]. In the case of 10 min milled composites with 60 vol.% Al_2O_3, the matrix phase support is decreased but not eliminated. This behavior is exhibited not only in compression but also in tension.

3.3 Density

Figure 10 demonstrates the relative density of the samples against Al_2O_3 content at different pressures. The liquid fraction of a composite depends not only on the forming temperature but also on the amount of reinforcement. As prescribed by the rule of mixtures, the theoretical density of the samples rises linearly with the increase of Al_2O_3 content [28]. As seen in Fig. 10, the measured relative density for high loading composites decreased by increasing Al_2O_3 volume fraction. It also shows lower experimental density compared with the theoretical density. The lower experimental density is due to the existence of porosity between reinforcements, which is not filled with the liquid phase. By increasing the reinforcement, the amount of the liquid phase decreased and the reinforcement hindered its penetration into the empty spaces. This leads to the clustering and agglomeration of Al_2O_3 particles. Therefore, higher compaction pressure increased the probability of liquid phase flow into the pores between the particles. The relative density of composites with high compaction pressure (100 MPa) is higher due to increased bonding and decreased porosity.

Irregularly shaped powders have high compressibility compared to the spherical ones [40]. Therefore, ball milling, which causes deformation of aluminum particles, affects the density of composites. Lack of compressibility of spherical particles and the inability of large alumina to penetrate between them caused 5 h milled composites with 40 vol.% Al_2O_3 to have the highest relative density. However, the agglomeration of this reinforcement at higher than 40 vol.% loading diminished the density and other mechanical properties, like hardness. The density of composites with 60 vol.% Al_2O_3 decreased for both types of milling powders. The reason is that the reinforcement volume increased, but on the other hand, the pressure contribution from the other phases decreased. Equation (1) shows the contribution of each phase to the total pressure of the punch [23]:

$$P_T = P_{Al2O3}\frac{A_{Al2O3}}{A_T} + P_{Al7075}\frac{A_{Al7075}}{A_T} \quad (1)$$

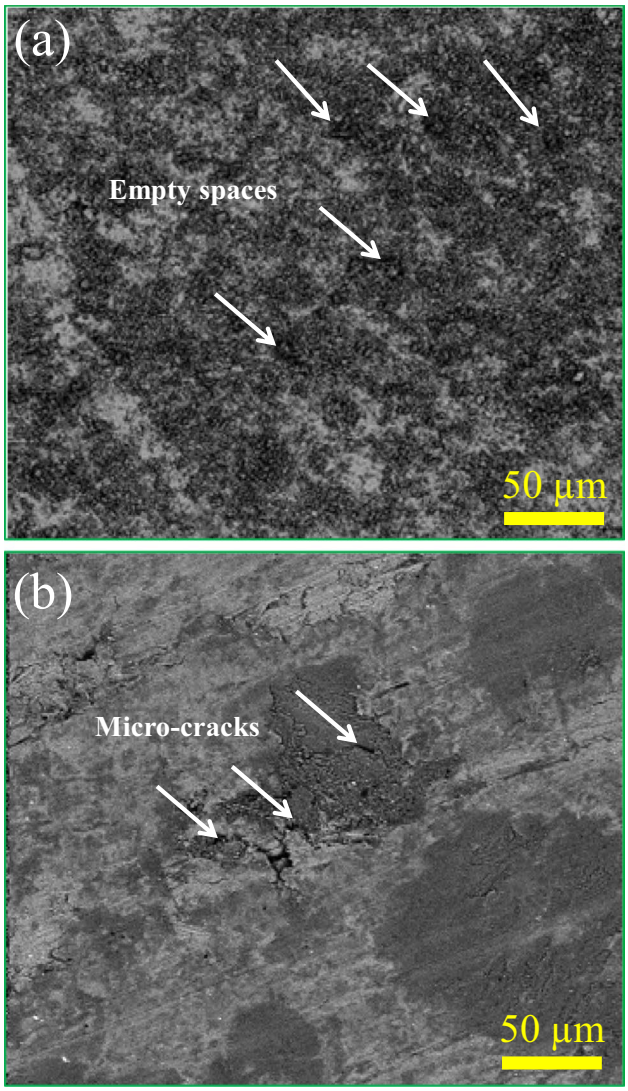

Fig. 9 The microstructure of 60 vol.% Al_2O_3 content: **a** 5 h milled and **b** 10 min milled composites

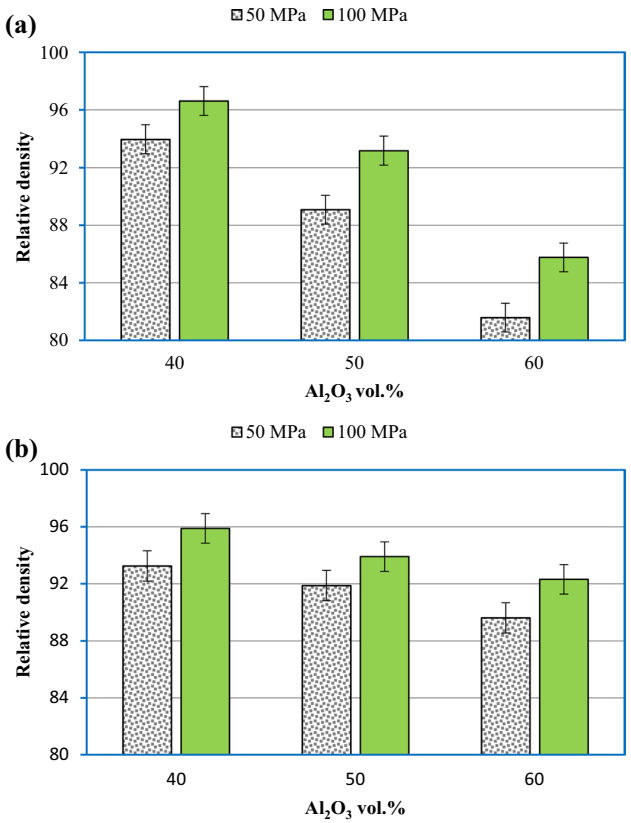

Fig. 10 Variation of relative density with the reinforcement volume fraction and semisolid compaction pressure for **a** 5 h milled and **b** 10 min milled composite powder

Here, P_T and A_T are the total pressure and the total contact area. P_{Al7075} and $P_{Al_2O_3}$ are pressure contributions from the Al_2O_3 and Al7075 phases, respectively. $A_{Al_2O_3}$ and A_{Al7075} are the contact areas between the punch and each phase. Since the pressure from pores is negligible, it is not considered in the equation. At constant pressure, it is observed that degrading the area of reinforcement particles is in accordance with the increase of the supporting pressure by this phase. Therefore, with increasing the reinforcement particles size, the pressure contribution of the soft matrix phase increased, providing the driving force for this phase to fill the porosity.

There are three different contact cases that can occur for the mixture of Al7075 and Al_2O_3 powders: between Al7075 and Al7075, Al7075 and Al_2O_3, and Al_2O_3 and Al_2O_3 particles. Among these cases, the contact between Al_2O_3 and Al_2O_3 particles can result in bonding between them as these particles cannot deform plastically. This can cause the formation of clusters or long-range network of Al_2O_3 that inhibits densification. By increasing the volume fraction of Al_2O_3 reinforcement, the probability of contact between Al_2O_3 particles increases. Consequently, the relative density of composites decreased by increasing the volume percentage of Al_2O_3 particles (Fig. 10).

3.4 Hardness and compressive strength

The effects of powder preparation and compaction pressure on the Vickers hardness of high loading composites were studied using the SCTMC micro Vickers hardness tester model HV-1000 by applying 5 N load and holding it for 15 s. The reported values are shown in Fig. 11a, representing the average of 4 measurements. The highest hardness pertains to 5 h milled 40 vol.% fraction-loaded composites compacted at 100 MPa. Contact area, which is a significant factor of composites' mechanical properties [41], is improved for fragmented particles and enhances the bond strength. Thus, at the same volume fraction, the hardness of composites with small reinforcements is higher than the hardness with

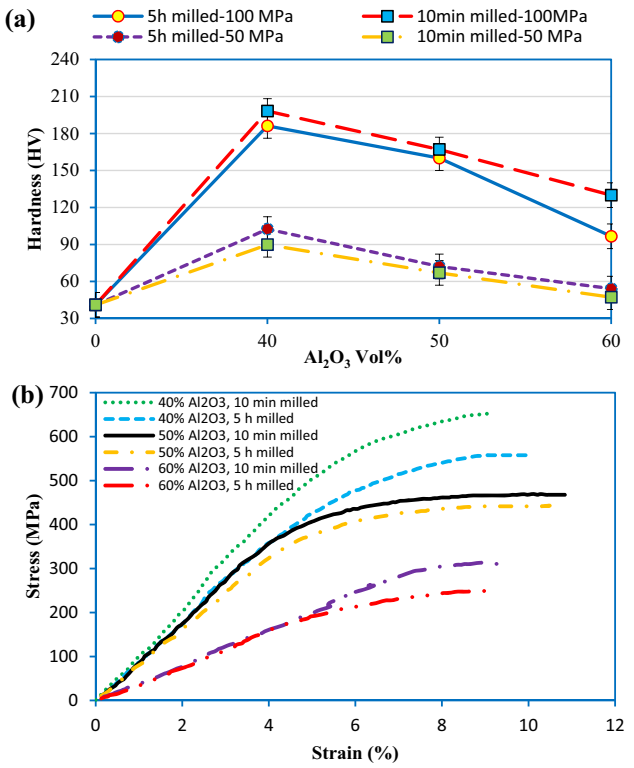

Fig. 11 **a** The hardness at various experimental conditions and **b** the compressive curves under 100 MPa pressure at 615 °C

the large ones. However, by increasing the Al_2O_3 loading to 50 vol.% and 60 vol.% fraction, hardness reduction was observed, which is another criterion for the lack of loading limits of these composites.

By increasing the compaction pressure from 50 to 100 MPa, the hardness values significantly increased for all samples. Increasing the applied pressure facilitates the liquid phase that will greatly accommodate solidification shrinkages and will fill pores and gaps within the powder mixture which results in the improvement of hardness values.

Opposite to the rule of mixtures, the hardness decreased by increasing reinforcement volume fraction in high loading composites. It is observed that the hardness decreased almost linearly with increasing the Al_2O_3 volume for both kinds of samples, whereas, for the 100 MPa compacted composites, the reduction only accelerates for the 60 vol.% fraction milled for 5 h. This reduction is also sharp for all the 50% and 60% reinforced samples. Good distribution of Al_2O_3 particles in the matrix phase hinders the generation of local hardness. For these composites, the local hardness was observed as a result of the particles interlocking and the decrease of matrix phase load support. These metal matrix composites are mentioned as overloaded composites. As a result, the aggregation of the two opposite features of increasing volume fraction and decreasing density causes a minor growth in composites' hardness compared with the unreinforced alloy.

Compression tests were performed to inspect the effects of milling time and semisolid compaction pressure on the mechanical properties of the Al7075-40 vol.% Al_2O_3 composite. All the samples were machined to the 12.7 mm diameter and 25.4 mm height and underwent compression test using Shimadzu AG-25 TB with a crosshead speed of 1 mm/min. The variation of compressive properties for 10 min and 5 h milled composites with 40 vol.% alumina content prepared at 50 MPa and 100 MPa is presented in Table 3. First, the effect of compaction pressure on compressive strength is considered, and it is concluded that samples compacted at 100 MPa exhibited a reasonable modulus of elasticity. This confirms the obvious effect of the compaction pressure in high loading composites. The results also showed that 10 min milled composites had higher strength than 5 h milled ones. Uniform distribution of the reinforcing particles within the matrix phase confirms this result in Fig. 7a.

The compression curves of the composites with different milling time (10 min and 5 h) prepared under 100 MPa are shown in Fig. 11b. The compressive strength decreased with increasing reinforcement content of more than 40 vol.% Al_2O_3. This might be the result of more aggregation of the reinforcing particles and the following porosity displayed at high loading composites. The compression response of samples milled for 10 min is superior to the samples containing small alumina particles as a result of long milling time of 5 h. This is due to the fact that tiny particles' barrier action led to poor bonding of the reinforcement and the matrix particles [42].

Flow curves from the compression tests for 60 vol.% alumina composites reveal more reduction in ultimate strength,

Table 3 Compressive strength and elastic modulus of the fabricated composites

Material		Elastic modulus (GPa)	Compressive strength (MPa)
Compacted at 50 MPa	10 min milled Al7075-40% Al_2O_3	81	218
	5 h milled Al7075-40% Al_2O_3	79	210
Compacted at 100 MPa	10 min milled Al7075-40% Al_2O_3	112	652
	5 h milled Al7075-40% Al_2O_3	108	549

especially in the case of 5 h milled samples. Debonding of the interface and decreased mechanical strength due to the difference in thermal expansion coefficients of particles are very common in the composites with high Al_2O_3 volume fraction [43]. As a result, the volume fraction of 60 vol.% Al_2O_3 is overloading for compaction pressure of 100 MPa.

All the specimens manifested brittle fracture behavior through surface examination. As shown in Fig. 11b, the ductility recorded for 5 h milled composites is higher than the 10 min milled ones. However, it is still low with a maximum amount of approximately 0.88% elongation recorded for the 5 h milled 40 vol.% Al_2O_3 composite. Despite this low amount of ductility, SPP provides higher elongation to fracture for high loading composites rather than other methods with almost similar materials demonstrated by Prater et al. [44] and Kouzeli et al. [45].

4 Conclusions

In this study, the mechanical characteristics of Al7075-Al_2O_3 composites prepared by semisolid processing and powder metallurgy were investigated. The conclusions are as follows:

1. The best mechanical properties of Al7075 powder with a relative density of 99.6% were obtained when the alloy is formed at the optimal reheating semisolid temperature of 615 °C. However, by increasing the temperature to 625 °C, the density slightly decreased to 99.3%.
2. The change in particles size was not very noticeable in the composites milled for 10 min while it was severely reduced for the composites milled for 5 h. By increasing the milling time, the large and brittle alumina particles fractured and aluminum particles experienced plastic deformation and flattening.
3. A uniform and homogenous distribution of the reinforcement particles among the matrix particles was achieved after 10 min milling. However, the uniformity was not evident after 10 min milling.
4. Different reinforcement distribution was identified for the SPP of Al7075/Al_2O_3 composites. In the compaction of composites milled for 10 min, the reinforcements were evenly distributed within the matrix phase without any changes in their morphology. For the composites milled for 5 h, the agglomeration of fragmented reinforcement particles was observed at grain boundaries of Al7075 grains after solidification.
5. After SPP processing, the maximum hardness of 198 HV and relative density of 96.9% were achieved for the composite with 40 vol.% reinforcement milled for 5 h. It was observed from the micrographs that the fragmentation of the reinforcing particles and their irregular shape improved the compressibility of reinforcement particles. The hardness and relative density of composites decreased by increasing the Al_2O_3 volume fraction to 50 vol.% and 60 vol.%.
6. The compaction pressure was key to SPP processing of Al7075-Al_2O_3 with high loadings of > 40%vol, so density, hardness and compression strength increased by increasing compaction pressure.
7. The compressive strength decreased with increasing reinforcement content. The volume fraction of 60 vol.% Al_2O_3 appeared overloading for compaction pressure of 100 MPa.

Funding The authors declare that there were no funds, grants, or other support were received for the preparation of this manuscript.

Data availability All data generated or analyzed during this study are included in this published article.

Declarations

Conflict of interest The authors declare no competing interests.

References

1. Pramod R, Veeresh Kumar GB, Gouda PSS, Mathew AT (2018) A study on the Al2O3 reinforced Al7075 metal matrix composites wear behavior using artificial neural networks. Mater Today Proc 5(5, Part 2):11376–11385
2. Awad M, Hassan NM, Kannan S (2021) Mechanical properties of melt infiltration and powder metallurgy fabricated aluminum metal matrix composite. Proc Inst Mech Eng B J Eng Manuf 235(13):2093–2107
3. Ramadoss N, Pazhanivel K, Ganeshkumar A, Arivanandhan M (2022) Microstructural, mechanical and corrosion behaviour of B4C/BN-reinforced Al7075 matrix hybrid composites. Inter Metalcast 17:499–514
4. Miserez A, Müller R, Rossoll A, Weber L, Mortensen A (2004) Particle reinforced metals of high ceramic content. Mater Sci Eng A 387:822–831
5. Chung D, Zweben C (2000) Composites for electronic packaging and thermal management. Comprehensive composite materials. Elsevier Science Ltd 6:701–725

6. Seleznev M, Cornie J, Mason R, Ryals M (1997) High volume fraction ceramic reinforced aluminum matrix composites for automotive applications: mechanical properties and microstructural characterization. Technical paper, MMCC Inc. Available from: www.mmccinc.com
7. Surappa MK (2003) Aluminium matrix composites: challenges and opportunities. Sādhanā 28(1):319–334
8. Clyne T, Kelly A, Zweben C (2000) Comprehensive composite materials. Metal matrix composites. Pergamon Oxford 3:1–26
9. Torquato S, Haslach H Jr (2002) Random heterogeneous materials: microstructure and macroscopic properties. Appl Mech Rev 55(4):B62–B63
10. Muraliraja R, Arunachalam R, Al-Fori I, Al-Maharbi M, Piya S (2019) Development of alumina reinforced aluminum metal matrix composite with enhanced compressive strength through squeeze casting process. Proc Inst Mech Eng L J Mater Des Appl 233(3):307–314
11. Wei S et al (2020) Correction to: Network-strengthened Ti-6Al-4V/(TiC+TiB) composites: powder metallurgy processing and enhanced tensile properties at elevated temperatures. Metall Mater Trans A 51(3):1437–1437
12. Gul F, Acilar M (2004) Effect of the reinforcement volume fraction on the dry sliding wear behaviour of Al–10Si/SiCp composites produced by vacuum infiltration technique. Compos Sci Technol 64(13–14):1959–1970
13. Kawasaki A, Watanabe R (1997) Concept and P/M fabrication of functionally gradient materials. Ceram Int 23(1):78–83
14. Lin C-Y, Bathias C, McShane HB, Rawlings RD (1999) Production of silicon carbide Al 2124 alloy functionally graded materials by mechanical powder metallurgy technique. Powder Metall 42(1):29–33
15. Parras-Medécigo E, Pech-Canul MI, Rodríguez-Reyes M, Gorokhovsky A (2002) Effect of processing parameters on the production of bilayer-graded Al/SiCp composites by pressureless infiltration. Mater Lett 56(4):460–464
16. Mazahery A et al (2012) Hardness and tensile strength study on Al356–B4C composites. Mater Sci Technol 28(5):634–638
17. Sajjadi SA, Ezatpour HR, Beygi H (2011) Microstructure and mechanical properties of Al–Al2O3 micro and nano composites fabricated by stir casting. Mater Sci Eng A 528(29):8765–8771
18. Jiang W et al (2021) Enhanced mechanical properties of 6082 aluminum alloy via SiC addition combined with squeeze casting. J Mater Sci Technol 88:119–131
19. Zhu J et al (2020) Microstructure and mechanical properties of SiCnp/Al6082 aluminum matrix composites prepared by squeeze casting combined with stir casting. J Mater Process Technol 283:116699
20. Ding H et al (2021) Enhancing strength-ductility synergy in an ex situ Zr-based metallic glass composite via nanocrystal formation within high-entropy alloy particles. Mater Des 210:110108
21. Grossi LJ, Reinke G, da Silva TC, Rosa DM, Muterlle PV (2021) Study of the influence of high-energy milling time on the Cu–13Al–4Ni alloy manufactured by powder metallurgy process. J Braz Soc Mech Sci Eng 43(1):44
22. Luo X, Wu M, Fang C, Huang B (2019) The current status and development of semi-solid powder forming (SPF). JOM 71(12):4349–4361
23. Wu Y, Kim G-Y, Anderson IE, Lograsso TA (2010) Fabrication of Al6061 composite with high SiC particle loading by semi-solid powder processing. Acta Mater 58(13):4398–4405
24. Javdani A, Pouyafar V, Ameli A, Volinsky AA (2016) Blended powder semisolid forming of Al7075/Al2O3 composites: investigation of microstructure and mechanical properties. Mater Des 109:57–67
25. Naseer A et al (2019) A review of processing techniques for graphene-reinforced metal matrix composites. Mater Manuf Process 34(9):957–985
26. Wu Y, Kim G-Y (2011) Compaction behavior of Al6061 powder in the semi-solid state. Powder Technol 214(2):252–258
27. Kok M (2005) Production and mechanical properties of Al2O3 particle-reinforced 2024 aluminium alloy composites. J Mater Process Technol 161(3):381–387
28. Tsai S (2018) Introduction to composite materials. Routledge
29. Hynes NRJ, Raja S, Tharmaraj R, Pruncu CI, Dispinar D (2020) Mechanical and tribological characteristics of boron carbide reinforcement of AA6061 matrix composite. J Braz Soc Mech Sci Eng 42(4):155
30. Rana R, Purohit R, Das S (2012) Review of recent studies in Al matrix composites. Int J Sci Eng Res 3(6):1–16
31. Chen C, Yang C, Chao C (2005) A novel method for net-shape forming of hypereutectic Al–Si alloys by thixocasting with powder preforms. J Mater Process Technol 167(1):103–109
32. Steinhoff K, Ursula W, Jan W (2004) Micro semi-solid manufacturing-a new technological approach towards miniaturisation. Steel Res Int 75:611–619
33. Chen YS, Chen TJ, Fu W, Li PB (2013) Microstructural evolution during partial remelting of 6061 aluminum bulk alloy prepared by cold-pressing of alloy powder. In Advanced Materials Research. Trans Tech Publ
34. Chen Y-s, Chen T-j, Zhang S-q, Li P-b (2015) Effects of processing parameters on microstructure and mechanical properties of powder-thixoforged 6061 aluminum alloy. Trans Nonferrous Met Soc China 25(3):699–712
35. Kim W, Kang C, Kim B (2007) The effect of the solid fraction on rheological behavior of wrought aluminum alloys in incremental compression experiments with a closed die. Mater Sci Eng A 447(1–2):1–10
36. Prabhu B, Suryanarayana C, An L, Vaidyanathan R (2006) Synthesis and characterization of high volume fraction Al–Al2O3 nanocomposite powders by high-energy milling. Mater Sci Eng A 425(1):192–200
37. Kamrani S, Penther D, Ghasemi A, Riedel R, Fleck C (2018) Microstructural characterization of Mg-SiC nanocomposite synthesized by high energy ball milling. Adv Powder Technol 29(7):1742–1748
38. Kang Y-C, Chan SL-I (2004) Tensile properties of nanometric Al2O3 particulate-reinforced aluminum matrix composites. Mater Chem Phys 85(2–3):438–443
39. Wu Y (2011) Fabrication of metal matrix composite by semi-solid powder processing [PhD dissertation]. IowaState University, Ames
40. Nouri A, Sola A (2018) Metal particle shape: a practical perspective. Met Powder Rep 73(5):276–282
41. Bazilchuk M et al (2020) Contact area measurement of micron-sized metal-coated polymer particles under compression. Int J Mech Sci 165:105214
42. Sharma S, Nanda T, Pandey OP (2018) Effect of particle size on dry sliding wear behaviour of sillimanite reinforced aluminium matrix composites. Ceram Int 44(1):104–114
43. Vencl A et al (2010) Structural, mechanical and tribological properties of A356 aluminium alloy reinforced with Al2O3, SiC and SiC+graphite particles. J Alloy Compd 506(2):631–639
44. Prater WL (2006) Comparison of ceramic material effects on the flexural Weibull statistics and fracture of high volume fraction particle reinforced aluminum. Mater Sci Eng A 420(1):187–198
45. Kouzeli M, Weber L, San Marchi C, Mortensen A (2001) Influence of damage on the tensile behaviour of pure aluminium reinforced with ≥40 vol. pct alumina particles. Acta Mater 49(18):3699–3709